WCTE 2014 Quebec City Canada August 10-14
World Conference on Timber Engineering

EXPERIMENTAL AND NUMERICAL INVESTIGATION OF NOVEL STEEL-TIMBER-HYBRID SYSTEM

Pooja Bhat[1], Riasat Azim[2], Marjan Popovski[3], Thomas Tannert[4]

ABSTRACT: This paper summarises the experimental and numerical investigation conducted on the main connection of a novel steel-timber hybrid system called FFTT. The component behaviour of the hybrid system was investigated using quasi-static monotonic and reversed cyclic tests. Different steel profiles (wide flange I-sections and hollow rectangular sections) and embedment approaches for the steel profiles (partial and full embedment) were tested. The results demonstrated that when using an appropriate connection layout, the desired strong-column weak-beam failure mechanism was initiated and excessive wood crushing was avoided. A numerical model was developed that reasonably reflected the real component behaviour and can subsequently be used for numerical sensitivity studies and parameter optimization. The research presented herein serves as a precursor for providing design guidance for the FFTT system as an option for tall wood-hybrid buildings in seismic regions.

KEYWORDS: Strong-column weak-beam failure mechanism, cross-laminated-timber, energy dissipation

1 INTRODUCTION

1.1 TIMBER IN MID- HIGH-RISE STRUCTURES

Numerous mid-rise wood-based structures have been built across Canada at the beginning of the 20th century. Some fire incidents in timber buildings during that period, however, were used to place severe area and height restrictions for buildings of combustible construction that remain to this day in Part 3 of the National Building Code of Canada (NBCC) [1].

In 2009, the British Columbia Building Code (BCBC) [2] allowied 6-storey light-frame wood construction and specified the maximum building height as 18m from the ground to the floor of the uppermost storey. These changes together with the recent introduction of innovative wood-based products and systems have revived the interest in extending the application of wood-based products from low-rise to mid-rise and potentially high-rise construction.

Engineered wood products (EWPs) provide engineers with alternative materials that possess efficient structural properties but also better environmental attributes compared to other construction materials. One of the key EWPs that provide this opportunity is Cross-Laminated Timber (CLT), a mass timber product developed in Europe in the 1990's. CLT is increasingly gaining popularity in residential and non-residential applications in Canada [3].

Extensive research has been conducted at FPInnovations [3] to study the behaviour of CLT and recommend changes to the current restrictions placed on the wood buildings in Canada. Many other studies conducted worldwide, e.g. [3-5] confirmed the high influence of the joints on the overall behaviour of a CLT structure, showing good seismic performance when using ductile conenctors.

According to the objective-based design approach in the 2010 NBCC version of, new structural systems that are not defined in the code can be used as "alternative solutions", provided that the alternative solution provides the same level of performance as the "acceptable solution" specified in NBCC. The adoption of this objective based approach in Canada can favour large-scale wood construction if equivalent performance design can be demonstrated. Lack of technical information and design guidance on new ductile wood-based structural systems, however, has hindered the construction of timber high-rise buildings in seismically active regions of Canada.

[1] Pooja Bhat, Research Assistant, Civil Engineering, UBC Vancouver, Canada, Email: poojabhat@civil.ubc.ca

[2] Riasat Azim, Research Assistant, Civil Engineering, UBC Vancouver, Canada, Email: riasat@civil.ubc.ca

[3] Marjan Popovski, Principal Scientist, FPInnovations, Vancouver, Canada, Email: Marjan.Popovski@fpinnovations.ca

[4] Thomas Tannert, Assistant Professor, Wood Science and Civil Engineering, UBC Vancouver, Canada, Email: thomas.tannert@ubc.ca (corresponding author)

1.2 TIMBER-STEEL-HYBRID SYSTEMS

Steel and wood are two materials with different properties, but combining them in buildings a way that takes advantage of their inherent properties while diminishing their limitations, can result in structures with superior performance. Steel excels in tension, while wood behaves well in compression parallel to grain. While the load-deformation relationship of wood under compression is usually ductile, it tends to fail in brittle failure mode in tension. Timber members have high strength to weight ratio compared to steel and concrete ones resulting in lighter structures. Since earthquake forces are proportional to the weight of the building, timber based buildings are usually attract lower forces during an earthquake. Structural steel members can dissipate great amounts of energy under cyclic loads and thus, if designed efficiently, steel structures exhibit good ductile behaviour during an earthquake event. The performance of timber structures during a seismic event is highly dependent on the behaviour of the connections. Ductile connections can help dissipate the seismic input energy during an earthquake event. Steel structural elements used in wood-hybrid buildings can provide this ductility to the system, thus improving the overall seismic performance of the hybrid building. Moreover, combining steel and wood results in sustainable construction due to high recycle content of steel and low carbon footprint of wood.

1.3 FFTT SYSTEM

Over the last decade, several innovative hybrid systems were developed to promote the use of timber in large-scale construction [6-7]. One such system is '*Finding Forest Through Trees'*, abbreviated as FFTT system proposed by Michael Green and Eric Karsh, which provides unique timber and steel hybrid approach for construction of tall wood buildings [8]. It consists of mass timber wall panels such as CLT, LSL, or LVL as the vertical system that are anchored down using ductile hold downs or dampers and rigid (elastic) shear connectors. Steel beams are partially embedded into the panel faces that hold the walls together across openings, see Figure 1.

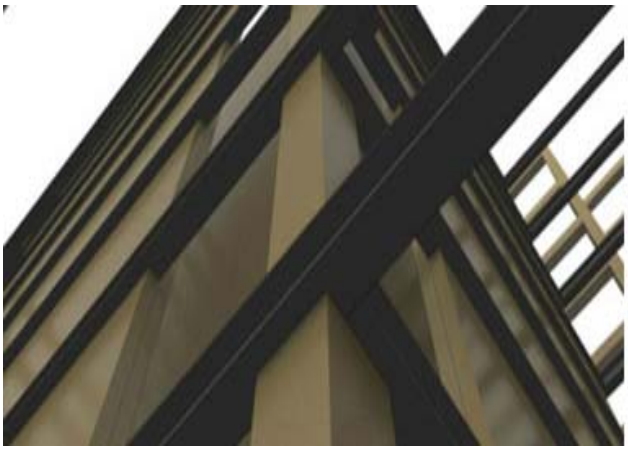

Figure 1: *Detail of the proposed FFTT system*

The force transfer for lateral loads occurs through the bearing of the header beams on the solid wood panels. The steel beams act as the ductile weak link of the system under lateral loads and are designed and detailed such that plastic hinging occurs at the beam sections triggering a "Strong–Column Weak–Beam" failure mechanism [8]. As in any system, the seismic design of FFTT requires careful balance of strength, stiffness, and ductility. Further structural analyses, testing and diligent peer review are necessary before the FFTT system can be successfully implemented in practice.

The experimental investigation carried out within the scope of the research presented in this paper addresses the interaction between the timber panel and embedded steel beam, embedment strength of the CLT panel, influence of cross-section profiles and placement of the embedded beams on the capacity and energy dissipation of the assembly under cyclic loads.

2 EXPERIMENTAL INVESTIGATIONS

2.1 SPECIMEN DESCRIPTION

Two 7-ply Spruce-Pine-Fir CLT panels, 3.9m long and 0.9m wide in combination with two beam profiles: i) wide flange I-section (150 x 100mm) and ii) hollow rectangular tube section (HSS, 100 x 50 x 3.1mm) were used in the tests. The beams were embedded into pre-cut slots in the panels and held in place using lag bolts.

In test series 1 and 2 that utilized wide-flange beams (I), the embedment depth was varied; for series 3, the cross section of the steel beam was reduced to induce yielding at a lower load level (Figure 2). Series 4 and 5 consisted of Hollow Structural Sections (HSS), the difference being the embedment length into the CLT panels. The main parameters of the five test series are presented in Table 1.

Table 1: *Summary of Test Series Configuration*

Series	Section	Embedment Length [mm]	Embedment Depth [mm]
1	I	900	50
2	I	900	100
3	Reduced I	900	100
4	HSS	900	50
5	HSS	600; 300	50

Figure 2: *Test specimen: series 1 (left) and 3 (right)*

2.2 METHODS

The CLT panels were bolted to the floor at both ends to restrain them from translation, rotation or uplift. The load was applied by means of a hydraulic actuator at the end of the projecting steel beam. Six sensors (labelled loc-1 to loc-6) along the steel beam allowed for measurement of the relative horizontal displacement between the beam and panel and the rotation of the steel beam (Figure 3).

Two replicates for each series were tested under quasi-static monotonic loading, while one specimen was tested under reversed cyclic loading. The static load was applied at a constant displacement rate according to EN-26891 [10]; the reversed cyclic tests followed the CUREE loading protocol according to ASTM E2126 [11].

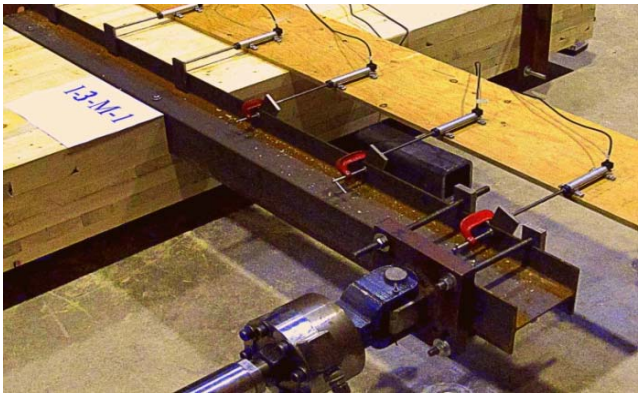

Figure 3: *Experimental setup for specimen from series 2*

2.3 RESULTS STATIC TESTS

The load-deformation relationship at the end of the embedded beam for each series is shown in Figure 4 showing the significant impact the steel profiles had.

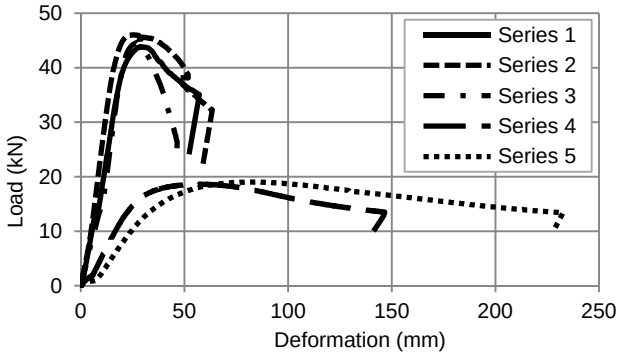

Figure 4: *Monotonic Tests: Load-Deformation Curves*

The interaction between timber and steel and the influence of embedment depth and reduced cross-section were also analysed. In all series that utilized I-section beams, the failure mode was ductile steel yielding accompanied with out-of-plane buckling of the beams. Rectangular hollow sections proved to be the better solution not only for reducing the out-of-plane buckling behaviour but also achieving ductile failure mechanisms without significant wood crushing even at partial embedment lengths.

During series 1 and series 2, the beam yielding occurred at the panel-beam interface at the exposed side of the top flange at an average load of 40kN and 41kN, respectively (Figure 5 a and b). The in-plane deformation of the beam caused negligible wood crushing, even at the interface. In series 3, beam yielding occurred at the point of cross-section reduction at the exposed side of the top flange at an average load of 44.5kN. Non-uniform yielding of the beam led the cantilever end to lift upwards after the beam had yielded near the interface (Figure 5 c). Significant uplift was observed, but the bolts had adequate uplift capacity and no wood crushing at the interface was observed.

For series 4 and 5, the beam yielding occurred at the beam-wall interface at an average load of 17kN (Figure 5 d and e). Due to uniform bearing of the HSS on the CLT panel, the yielding occurred symmetrically on both faces. Neither beam uplift nor withdrawal of lag bolt was seen. No wood crushing occurred around the embedded beam in the end grain of CLT, but wood deformation of 10mm was recorded at the interface in the layer with grain orientation perpendicular to the load during series 5 (Figure 5f).

2.4 RESULTS CYCLIC TESTS

The mode of failure during series 1 was pull-out of the beam from the embedded portion along with some wood failure instead of expected yielding at the interface (Figure 6 a and b). The lag bolts and the beam began withdrawing from the embedded position before the onset of beam yielding at the interface at a load of approximately 40kN. The loading was continued only until 70% of the target displacement, with 34 load cycles in total, at which point complete beam withdrawal from the panel occurred.

The first test of series 2 was conducted without restricting beam uplift. The cyclic load was continued until 38 load cycles, achieving 120% of target displacement and a load of 48kN. Since the actuator was not anchored, pull-out of the embedded beam did not occur until the beam had fully yielded (Figure 6 c and d). The second test was conducted with larger bolts to resist the beam from pulling out. The cyclic load was continued until 37 load cycles (100% of the target displacement) and a load of 52kN. Significant uplift was seen at the cantilever end and the bolt closest to the interface withdrew as the beam yielded and lifted from its embedded position (Figure 6 e). The embedded end of the beam, however, was held in place with the second lag bolt resisting the complete beam pull-out from the end.

The cyclic load for series 3 was continued until 36 load cycles, achieving 100% of target displacement and a load of 44kN. Significant uplift was observed at the end of the cantilever portion of the beam while the embedded end of the beam was held in place without any beam pull-out. The lag bolt closer to the interface did not display adequate withdrawal capacity and slight uplift of the beam was seen at the interface (Figure 6 f). The beam yielding occurred at the point of cross-section reduction and negligible wood damage (less than 4mm) was incurred due to in-plane beam deformation and beam uplift near the interface.

Figure 5: *Test specimens after static loads: (a) Beam Yielding Series 1; (b) Beam Yielding Series 2; (c) Beam Yielding and Uplift Series 3; (d) Beam Yielding Series 4; (e) Beam Yielding Series 5; (f) Wood Damage Series 5*

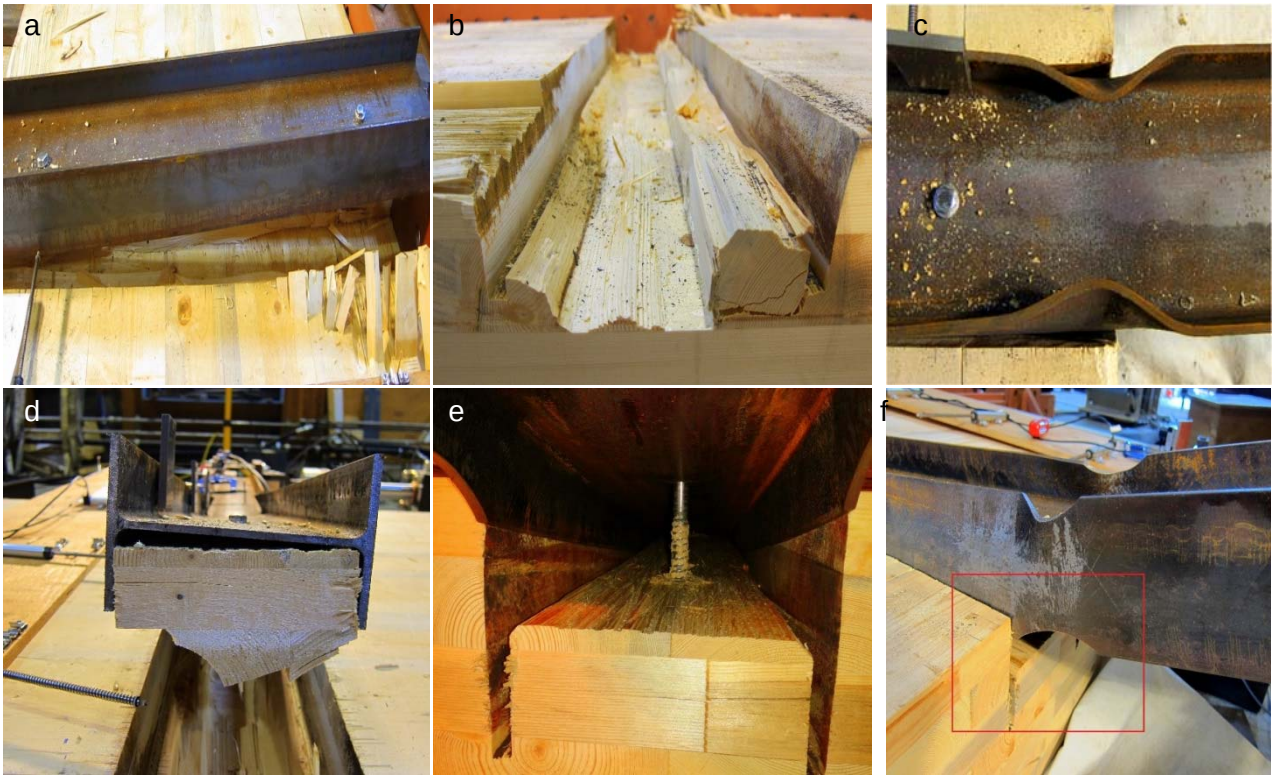

Figure 6: *Test specimens after cyclic loads: (a) Beam Pull-out Series 1; (b) Wood damage Series 1; (c) Beam yielding Series 2; (d) Beam Uplift Series 2; (e) Lag bolt withdrawal Series 2; (f) Beam Yielding and Uplift Series 3*

2.5 DISCUSSION

The obtained hysteresis loops were typical of a steel component, implying a connection with adequate ductility for the desired seismic application. A typical energy dissipation graph under cyclic load, shown in Figure 7, demonstrates that all energy is dissipated by the steel beam (LVDTs 4-6).

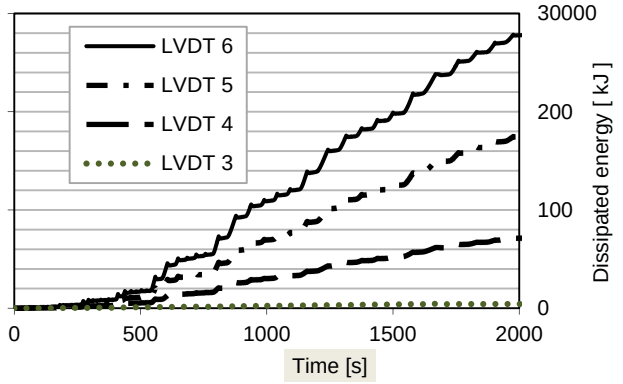

Figure 7: *Energy dissipation under cyclic loads (Series 5)*

Main parameters from monotonic and cyclic tests are summarized in Table 2. The ultimate deformation at the end of the beam is defined as the deformation at load equal to 80% of the peak load. The energy dissipation was calculated based on the area under the hysteresis curves obtained from the cyclic loads. The effect of embedment depth on the load carrying capacity and post-yield behaviour was negligible. The cross-section reduction of the beam facilitated a slightly more uniform yielding in the steel member and slightly increased the capacity.

Table 2: *Summary of Monotonic and Cyclic Test Results*

Series	Yield load [kN]	Ultimate displ. [mm]	Load cycles	Dissipated energy [J]
1	40.0	76.2	34	4,066
2	41.0	64.7	38	19,228
3	44.5	72.6	36	5,326
4	17.0	126.0	42	21,086
5	17.1	174.5	42	27,844

The beam profile had significant effect on the load-carrying capacity of the system. The I-sections were about 2.5 times stronger and 3 times stiffer than the HSS (the moment of inertia of the I-section was approximately 6 times larger than that of the HSS). The HSS retained a major proportion of their load-carrying capacity beyond the point of yielding and displayed a flatter post-yield curve (indicating more system ductility). The strength degradation beyond yielding in I-sections was rapid. The HSS possessed higher deformation capacity than I-sections. Due to the profile nature, the bearing of the HSS against the CLT panel was uniform causing beam yielding simultaneously on both sides of the section. The deformation was in-plane without beam twisting.

No considerable variation in the load-carrying capacity of HSS with different embedment lengths was observed. However, the decrease in the embedment length of the beam to 1/3 of the width of the panel increased the ultimate deformation capacity by 40%. More tests with different embedment lengths and beam placements are necessary to get a clear understanding of the effect of embedment on the post-yield behaviour of the system.

The location at which the deformation and dissipated energy was closest to zero was called the 'point of beam rotation'. The position of beam rotation (within the CLT panel) was calculated based on the load-displacement relationships of the LVDTs attached to the embedded beam section. The location about which the beam rotated in Series 1 and Series 3 was near the location of LVDT 2 (457mm from the interface) while the point of beam rotation for rest of the configurations (Series 2, 4 and 5) was about the location of LVDT 3 (152mm from the interface). These points are of great interest in the estimation of the stress transfer between steel and timber through the bearing of the embedded beams on the wall panels.

The behaviour under cyclic loads confirmed that the initiation of plastic hinge in the embedded beam section was the most significant contributing factor towards the system ductility. The CLT panels behaved as rigid members and resisted the in-plane wood deformation under the bearing of embedded steel sections, dissipating little energy. Almost all energy was dissipated through the in-plane deformation of the overhanging portion of the steel beams. The total energy dissipating capability of the system was dependent on number of cyclic deformation undergone by the embedded beam sections. Series 1 underwent the least amount of cyclic deformation before the brittle failure. The out-of-plane buckling of the cantilever side of the interface was more dominant under cyclic loads and thus, the in-plane deformation capacity of the system was greatly reduced. The eccentricity due to the non-symmetric beam yielding in series 2 and series 3 resulted in beam twisting at the interface. The out-of-plane buckling of the beam under cyclic loads increased the rate of strength degradation between the load cycles and decreased the in-plane deformation capacity of the system.

The hysteresis loops in the cyclic tests were large, implying a connection with adequate ductility for the desired seismic application. The dominant in-plane behaviour of the HSS made the system capable of undergoing larger cyclic deformations without a significant decrease in load bearing capacity. The hysteresis behaviour of the beam in the embedded portion was within the linear range and the nonlinearity in the system was contributed by the yielding at the interface and in-plane deformation of the cantilever portion of the beam. The stiffness of the system was reduced when the embedment length was decreased to 1/3 of the panel width and embedment allowed the beam to rotate more freely in the panel.

3 NUMERICAL INVESTIGATIONS

3.1 MODEL DEVELOPMENT

To complement the experimental results, a numerical investigation was carried out using ANSYS [12]. To model the CLT panels, SOLID186 elements were used; CLT was modelled a linear elastic orthotropic with the mechanical properties shown in Table 3. The x and y direction properties were altered to represent the different layers of CLT. The layers of CLT panels are glued together so that force transfer occurs between adjacent layers. SOLID 186 elements were also used to model the steel. Bilinear isotropic elasto-plastic material properties were applied to accommodate the post-yield inelastic response of the steel beam. The material properties were: elastic modulus E = 210000MPa, yield strength, fy = 310MPa; plastic stiffness α = 5000MPa; and ultimate strength, fu = 420 MPa.

Table 3: *CLT material properties used in the model*

Elastic Modulus [MPa]	Poisson Ratio	Shear Modulus [MPa]
E_x = 11,000	ν_{xy} = 0.40	G_{xy} = 700
E_y = 5,500	ν_{xy} = 0.40	G_{xz} = 500
E_z = 600	ν_{xy} = 0.04	G_{yz} = 70

Contact elements represented the gap and contact between the components; the coefficient of friction between steel and wood was set to 0.3. All degrees of freedom were constrained at the base and at the top of the CLT panel, and in the model, the steel beam was prevented against lateral buckling. A typical model is shown in Figure 8.

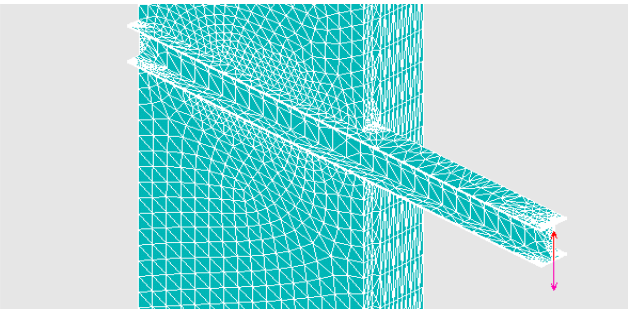

Figure 8: *Ansys model (Series 1)*

3.2 NUMERICAL RESULTS

The five different test configurations were modelled and a static pushover analysis for each test series was performed. For each configuration, the load-displacement curves at the locations of the six LVDTs were recorded and compared to those of the experimental results. The results for Series 1 and 4 are exemplarily shown in Figure 9.

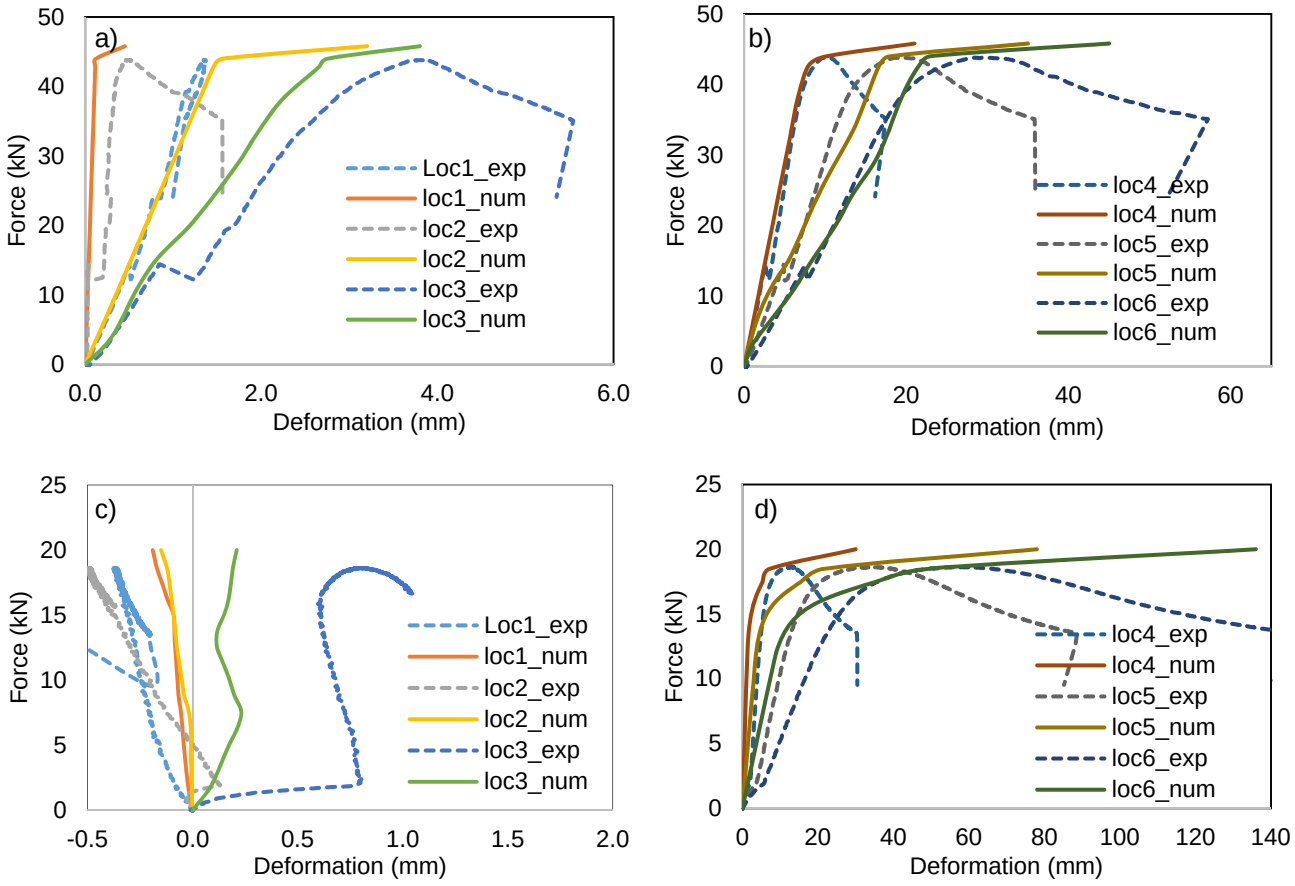

Figure 9: *Load-deformation plots comparing experimental and numerical results: (a) embedded portion series 1; (b) cantilever portion series 1; (c) embedded portion series 4; (d) cantilever portion series 4*

For the I section, it can be observed that the deformations inside the CLT panel were very small (<3mm), while the maximum displacement was computed as 46mm at the free end of the beam. The configurations with HSS sections (series 4) showed smaller displacements due to the lower applied load: from the numerical analysis, the maximum displacement inside the CLT panel was <1mm and at the free end of the beam 138mm. While the shape of the curve for the cantilever portion matches with the experiment; this is not the case for the embedded portion. Similar to the configuration 1 and 4, other configurations were also modelled and analysed and similar agreement between the numerical and experimental load-displacement curves was obtained. Therefore, it can be concluded that the numerical model reasonably reflects the real component behaviour and can subsequently be used for numerical sensitivity studies and parameter optimization.

4 CONCLUSIONS

The research focused on the component level performance of the proposed hybrid FFTT system under quasi-static monotonic and reversed cyclic loads. The effects of partial embedment, cross-section reduction, embedment length and the beam profile were investigated. A full-size 7-ply CLT assembly subjected to static and cyclic loads demonstrated high connection strength while maintaining ductile performance. The embedment of steel sections in the CLT wall panels increased the deformation capacity of the structure under lateral loads and significantly increased the ductility of the system. Most of the energy dissipation occurred as a result of the in-plane deformation of the cantilever portion of the embedded beam while the embedded portion were held in the wall panel by means of simple bolted connections. The embedded steel beams initiated the desired ductile 'Strong Column – Weak Beam' failure mechanism by beam yielding at the intersection of the wood panel and the steel beam.

ACKNOWLEDGEMENTS

This research was supported by the Natural Sciences and Engineering Research Council of Canada (NSERC) and the Wood First Program by Forestry Innovation Investments. The support from Johannes Schneider and Paul Simmons (FPInnovations) is acknowledged. The CLT panels were provided by Structurlam Products LP.

REFERENCES

[1] National Building Code of Canada (NBCC). National Research Council Canada, Ottawa, Canada, 2010.

[2] Building Code of British Columbia (BCBC). Crwon Publications, Victoria, Canada, 2012.

[3] Gagnon S, Pirvu C (2011) Cross Laminated Timber Handbook. FPInnovations, Vancouver, Canada.

[4] Ceccotti A, Sandhaas C, Yasumuro M (2010). Seismic Behaviour of Multistory Cross-Laminated Timber Buildings. International Convention of Society of Wood Science and Technology, Genewa, Switzerland.

[5] Popovski M, Schneider J, Schweinsteiger M (2010) Lateral load resistance of cross-laminated wood panels. World Conference on Timber Engineering, Riva del Garda, Italy.

[6] Skidmore, Owings & Merrill, LLP (2013) Timber Tower Research Project: Final Report

[7] Professner H, Mathis C (2012) LifeCycle Tower-High-Rise Buildings in Timber. ASCE Structures Congress, Chicago, USA

[8] Green MC, Karsh JE (2012) TALL WOOD - The case for tall wood buildings. Vancouver: Wood Enterprise Coalition.

[9] Bhat P (2013) Experimental investigation of connection for the FFTT timber-steel hybrid system. MASc thesis, University of British Columbia, Vancouver, Canada.

[10] EN-26891 (1991) Timber structures, Joints made with mechanical fasteners, General principles for the determination of strength and deformation characteristics. CEN European Committee for Standardization, Brussels, Belgium.

[11] ASTM E2126-11 (2013) Standard Test Methods for Cyclic (Reversed) Load Test for Shear Resistance of Vertical Elements of the Lateral Force Resisting Systems for Buildings, ASTM International, West Conshohocken, USA.

[12] ANSYS 14.5. 2012 SAS IP, Inc.